THE JOURNAL OF BIOLOGICAL CHEMISTRY
Vol. 279, No. 38, Issue of September 17, pp. 39268–39278, 2004
Printed in U.S.A.

Oxidative Stress-induced Apoptosis in Retinal Photoreceptor Cells Is Mediated by Calpains and Caspases and Blocked by the Oxygen Radical Scavenger CR-6*

Received for publication, February 27, 2004, and in revised form, May 26, 2004
Published, JBC Papers in Press, June 21, 2004, DOI 10.1074/jbc.M402202200

Nuria Sanvicens‡§, Violeta Gómez-Vicente‡§, Isabel Masip¶, Angel Messeguer¶, and Thomas G. Cotter‡‖

From the ‡Tumour Biology Laboratory, Department of Biochemistry, Bioscience Research Institute, University College, Cork, Ireland and the ¶Department of Biological Organic Chemistry, Institut d'Investigacions auímiques i Ambientals de Barcelona, Consejo Superior de Investigaciones Científicas, Jordi Girona 18-26, 08034 Barcelona, Spain

A critical role for reactive oxygen species (ROS) in photoreceptor apoptosis has been established. However, the exact molecular mechanisms triggered by oxidative stress in photoreceptor cell death remain undefined. This study delineates the molecular events that occur after treatment of the photoreceptor cell line 661W with the nitric oxide donor sodium nitroprusside (SNP). Cytosolic calcium levels increased during photoreceptor apoptosis, leading to activation of the calcium-dependent proteases calpains. Furthermore, caspase activation also occurred following SNP insult. However, although treatment with the pan-caspase inhibitor benzyloxycarbonyl-Val-Ala-Asp fluoromethyl ketone inhibited caspase activity *per se* in SNP-treated 661W cells, it did not prevent apoptosis. On the other hand, CR-6 (3,4-dihydro-6-hydroxy-7-methoxy-2,2-dimethyl-1(2*H*)-benzopyran) acted as a scavenger of ROS and reduced 661W photoreceptor apoptosis induced by SNP by preventing the activation of a pathway in which calpains have a key role. In summary, we report for the first time that both caspases and calpains are involved in 661W photoreceptor apoptosis and that calpain activation can be prevented by the ROS scavenger CR-6.

The cell death process of apoptosis is characterized by a series of morphological and biochemical changes, including membrane blebbing, loss of plasma membrane asymmetry, chromatin cleavage, and DNA fragmentation (1, 2). Apoptosis plays a central role in tissue modeling during development and, together with the cell-generating process of mitosis, is responsible for the maintenance of cell numbers in multicellular organisms. Deregulation of apoptosis has been well documented in several human pathologies, including cancer, neurodegenerative diseases, and AIDS (3, 4). Apoptosis also appears to be responsible for the cell loss seen in several disorders of the retina, including retinitis pigmentosa (a heterogeneous group of inherited disorders), glaucoma, and macular degeneration (5–8). Experiments aimed at unraveling the signaling pathways of apoptosis have identified several distinct mechanisms, and it has largely been accepted that caspases play a key role in both the initiation and execution pathways of apoptosis. However, the involvement of caspases does not seem to be clear-cut in some tissue systems. For example, there is still considerable controversy as to whether caspases play a role in retinal cell death (9–12). There is also some uncertainty about the role of caspases in neurodegenerative conditions (13–15). Recent work from our laboratory has indicated that photoreceptor death in animal models of retinitis pigmentosa proceeds in the absence of caspase activity, suggesting a caspase-independent mechanism of cell destruction (11, 12, 16). The exact mechanisms operating in photoreceptor death are still unclear but may involve calpains rather than caspases as the executing enzymes. These studies also suggested a key role for reactive oxygen species (ROS)[1] and reactive nitrogen intermediates (RNI) since inhibitors of nitric-oxide synthase blocked the cell death seen. These results are quite interesting since several studies have indicated that the eye is particularly sensitive to oxidative stress and therefore, modifications of the cellular redox state of the eye have been reported to play an important role in retinal degeneration processes (17–20). Additional support for the involvement of ROS and oxidative stress in photoreceptor apoptosis comes from several studies in which antioxidants appeared to retard or inhibit the degenerative pathology (21–23). However, the mechanisms of action of these anti-apoptotic molecules are unclear, and further work is necessary to resolve whether oxidative stress acts as a common mediator of retinal degeneration in retinitis pigmentosa.

The retina is composed of several different cell types, and this complicates any studies aimed at delineating the underlying mechanism of photoreceptor apoptosis. The production and characterization of the photoreceptor cell line 661W by Al-Ubaidi *et al.* (24) have greatly facilitated work in this area. This cell line expresses several markers of photoreceptors and has proved useful for *in vitro* studies investigating photoreceptor apoptosis (19, 20, 25, 26). In the context of this work, we have used this cell line to investigate the role played by oxidative stress in photoreceptor apoptosis induced by the nitric oxide donor sodium nitroprusside (SNP). This constitutes a direct extension of previous work from this laboratory (11) in which we showed that nitric oxide and ROS play a key role in driving

* This work was supported by the European Union, Fighting Blindness Ireland, and the Higher Education Authority of Ireland. The costs of publication of this article were defrayed in part by the payment of page charges. This article must therefore be hereby marked "*advertisement*" in accordance with 18 U.S.C. Section 1734 solely to indicate this fact.

§ Both authors contributed equally to this work.
‖ To whom correspondence should be addressed. Tel.: 353-21-490-1321; Fax: 353-21-490-1377; E-mail: t.cotter@ucc.ie.

[1] The abbreviations used are: ROS, reactive oxygen species; RNI, reactive nitrogen intermediates; SNP, sodium nitroprusside; Z-VAD-fmk, benzyloxycarbonyl-Val-Ala-Asp fluoromethyl ketone; PARP, poly(ADP-ribose)polymerase; Ac-DEVD-*p*NA, acetyl-Asp-Glu-Val-Asp *p*-nitroanilide; PBS, phosphate-buffered saline; RNI, reactive nitrogen intermediate(s); DHE, dihydroethidium; CHAPS, 3-[(3-cholamidopropyl)dimethylammonio]-1-propanesulfonic acid; ER, endoplasmic reticulum.

photoreceptor apoptosis *in vivo*. In this study, we show that SNP induced ROS production in the mitochondrion and that this in turn triggered apoptosis, with both calpains and caspases playing a role. Treatment with the pan-caspase inhibitor benzyloxycarbonyl-Val-Ala-Asp fluoromethyl ketone (Z-VAD-fmk) inhibited the activation of caspases, but does not appear to be a useful strategy to prevent oxidative stress-induced apoptosis in 661W photoreceptor cells. On the other hand, in the context of this work, we show that CR-6 (a vitamin E analog that has been shown to prevent glutamate neurotoxicity in cultured neurons due to its role as a nitric oxide scavenger (27)), interfered with oxidative stress-induced apoptosis in 661W cells by preventing the activation of the calpain-mediated apoptotic pathway.

EXPERIMENTAL PROCEDURES

Drugs, Reagents, and Antibodies—SNP was purchased from Sigma (Poole, United Kingdom). The synthesis of CR-6 has been described elsewhere (28). Cell Signaling Technology (Beverly, MA) provided anti-poly(ADP-ribose) polymerase (PARP) (catalog no. 9542), anti-caspase-3 (catalog no. 9662), anti-caspase-9 (catalog no. 9504), and anti-caspase-12 (catalog no. 2202) antibodies. Anti-Calpain-1 (catalog no. 208753) and anti-calpain-2 (catalog no. 208755) antibodies were purchased from Calbiochem. Anti-calpastatin (sc-7561) and anti-calpain small regulatory subunit (C-20; sc-7528) antibodies were from Santa Cruz Biotechnology (Santa Cruz, CA). Anti-β-actin antibody was from Sigma. Peroxidase-conjugated anti-rabbit, anti-goat, and anti-mouse secondary antibodies were obtained from Dako Corp. The broad-spectrum caspase inhibitor Z-VAD-fmk was purchased from Bachem Ltd. (Meyerside, United Kingdom). Alexis Co. (Läufefingen, Switzerland) provided the caspase-3 substrate acetyl-Asp-Glu-Val-Asp *p*-nitroanilide (Ac-DEVD-*p*NA).

Cell Culture—661W cells were kindly provided by Muayyad Al-Ubaidi, Department of Cell Biology, University of Oklahoma (Oklahoma City, OK). 661W cells were routinely grown in Dulbecco's modified Eagle's medium supplemented with 10% heat-inactivated fetal calf serum (both from Sigma) and 1% penicillin/streptomycin at 37 °C in a humidified 5% CO_2 atmosphere as described (20). SNP was used to induce apoptosis at the doses indicated; SNP stock was prepared at 100 mM in phosphate-buffered saline (PBS) (pH 7.4). Pretreatment of 661W photoreceptors with CR-6 was done for 15 min at 37 °C as described above. A 100 mM CR-6 stock was prepared in Me_2SO. Treatments carried out in 6-well plates (Nalge Nunc International, Hereford, United Kingdom) were as follow. Cells (75×10^4/well) were seeded and allowed to attach for 20 h at 37 °C. Following insult, cells were detached with a trypsin/EDTA solution (Sigma) and collected together with their supernatants for flow cytometric analysis. Cells for Western blot analysis were grown in 75-cm^2 flasks (Sarstedt AG & Co., Nümbrecht, Germany). Initially, cells (8×10^5/flask) were seeded and allowed to attach before treatment. Samples were collected 24 or 48 h post-insult.

Analysis of Generated RNI: Griess Reaction—Determination of the presence of RNI was done by means of the Griess reaction (29). Briefly, cells (5×10^4) were incubated for 15 min in the dark at room temperature with 40 μl of Griess reagent (Alexis Corp.). Nitrites present in the samples react with sulfanilic acid and *N*-(1-naphthly)ethylenediamine dihydrochloride in the presence of phosphoric acid, which produces a colored azo dye that can be measured at 548 nm.

Analysis of Intracellular ROS Generation—Measurement of superoxide anion levels was carried out as described previously (30). Briefly, cells were loaded with 10 μM dihydroethidium (DHE) (Molecular Probes, Inc., Leiden, The Netherlands), prepared from a 10 mM stock in Me_2SO, for 15 min at 37 °C. Superoxide anion oxidizes DHE intracellularly to produce ethidium bromide, which fluoresces upon interaction with DNA. The fluorescence due to ethidium bromide in a BD Biosciences FACScan flow cytometer with excitation and emission settings of 488 and 590 nm, respectively, was monitored to assess superoxide anion levels. CellQuest software was used for data analysis, and 10,000 events/sample were acquired.

Cell Death Measurement—Propidium iodide (Sigma) was used to quantify cell death. Treated cells were collected as described above, washed once with ice-cold PBS, and resuspended to a final concentration of 1×10^5 cells/ml. Propidium iodide (50 μg/ml) was added immediately before flow cytometric analysis. Fluorescence was measured at FL2 (590 nm), and 10,000 events/sample were acquired.

Measurement of Intracellular Free Ca^{2+}—Intracellular Ca^{2+} levels were determined using the intracellular Ca^{2+} probe Fluo-3/acetoxymethyl ester (Molecular Probes, Inc.), which binds Ca^{2+} with a 1:1 stoichiometry. After trypsinization, cells were washed once with PBS and resuspended in fresh buffer. Cells were incubated in the darkness with 250 nM Fluo-3, prepared from a 500 μM stock, for 30 min at 37 °C. Fluorescence was measured at FL1 (530 nm) in a BD Biosciences FACScan flow cytometer with excitation at 488 nm, and CellQuest software was employed for subsequent data analysis. At least 10,000 events/sample were acquired.

Western Blot Analysis—After exposure to drug, whole cell extracts were obtained and resolved by denaturing SDS-PAGE. Briefly, harvested cells were washed twice with ice-cold PBS; resuspended in cell lysis buffer (50 mM Tris-HCl (pH 7.4), 150 mM NaCl, 1 mM Na_3VO_4, 1 mM NaF, 1 mM EGTA, 1% Nonidet P-40, and 0.25% sodium deoxycholate) containing antipain (1 μg/ml), aprotinin (1 μg/ml), chymostatin (1 μg/ml), leupeptin (0.1 μg/ml), pepstatin (1 μg/ml), and 0.2 mM 4-(2-aminoethyl)benzenesulfonyl fluoride; and incubated on ice for 20 min. Supernatants were recovered by a 10-min centrifugation ($10{,}000 \times g$) at 4 °C, and protein concentration was determined with the Bio-Rad protein assay using bovine serum albumin as a standard. Proteins (20–40 μg) were diluted in 2× sample buffer (10% SDS and 100 mM each dithiothreitol, glycerol, bromphenol blue, and Tris-HCl) and resolved on 6–12% SDS-polyacrylamide gels. Then proteins were transferred onto nitrocellulose membranes (Schleicher & Schüll, Dassel, Germany), and the blots were blocked with 5% (w/v) nonfat dry milk in Tris-buffered saline and 0.1% Tween 20 for 1 h at room temperature. Membranes were incubated overnight at 4 °C with the appropriate dilution of primary antibody (1:5000 for anti-m-calpain and anti-μ-calpain antibodies and 1:1000 for all other antibodies). After three 5-min washes with Tris-buffered saline and 0.1% Tween 20, the blots were incubated with the corresponding peroxidase-conjugated secondary antibody (1:1000 dilution) for 1 h at room temperature. They were then washed again three times with Tris-buffered saline and 0.1% Tween 20, rinsed briefly with PBS, and developed with enhanced chemiluminescence reagents (ECL, Amersham Biosciences, Buckinghamshire, United Kingdom). Detection of β-actin (1:5000 antibody dilution) was used as control for equal loading of protein.

Determination of Ac-DEVD-pNA Cleavage—661W cells (8×10^5) were grown in 75-cm^2 flasks and preincubated at 37 °C with the caspase inhibitor Z-VAD-fmk (50 μM) for 1 h prior to insult with 0.3 mM SNP. Untreated and 0.3 mM SNP-treated 661W cells were used as negative and positive controls, respectively. After a 24-h incubation, cells were collected as described above and centrifuged at $500 \times g$ for 5 min. The pellet was resuspended in 1 ml of ice-cold 1× PBS and transferred to a microcentrifuge tube. Subsequently, the pellet was resuspended in 50 μl of ice-cold lysis buffer (100 mM HEPES (pH 7.4), 1 M NaCl, 1% CHAPS, 1 M dithiothreitol, 10 mM EDTA, and 1% Nonidet P-40) and incubated on ice for 10 min. Following a 20-s sonication, cell lysates were centrifuged for 10 min at $12{,}500 \times g$. The protein content of each sample was determined by the Bio-Rad protein assay using bovine serum albumin as a standard. An equal quantity of protein (50 μg) was loaded into each well of a microtiter plate, and the final volume was made up to 90 μl with assay buffer (same as lysis buffer minus 1% Nonidet P-40). Lysates were incubated with 0.2 mM Ac-DEVD-*p*NA at 37 °C for 20 h. Cleavage of the peptide substrate DEVD-*p*NA was monitored by liberation of chromogenic *p*NA in a SpectraMax-340 plate reader (Molecular Devices, Menlo Park, CA) by measuring absorption at 405 nm.

Annexin V Assay—A combined staining with fluorescein isothiocyanate-conjugated annexin V and propidium iodide was performed as a measure of apoptosis. Harvested cells were washed once with Ca^{2+} binding buffer (10 mM HEPES (pH 7.4), 140 mM NaCl, and 2.5 mM $CaCl_2$) and resuspended in 100 μl of the same buffer containing fluorescein isothiocyanate-conjugated annexin V (IQ Products, Groningen, The Netherlands). After a 15-min incubation in the dark at room temperature, cells were diluted with 400 μl of binding buffer, and propidium iodide was added before flow cytometric analysis. Fluorescence was measured as described above.

RESULTS

SNP Induces ROS Production and Cell Death in the Photoreceptor Cell Line 661W—Oxidative stress has been reported to play an important role in photoreceptor cell death (18, 20). Previous work carried out in this laboratory demonstrated that nitric oxide mediates retinal degeneration *in vivo* and that ROS significantly contribute to photoreceptor cell death (11). Despite these findings, the mechanisms leading to photoreceptor

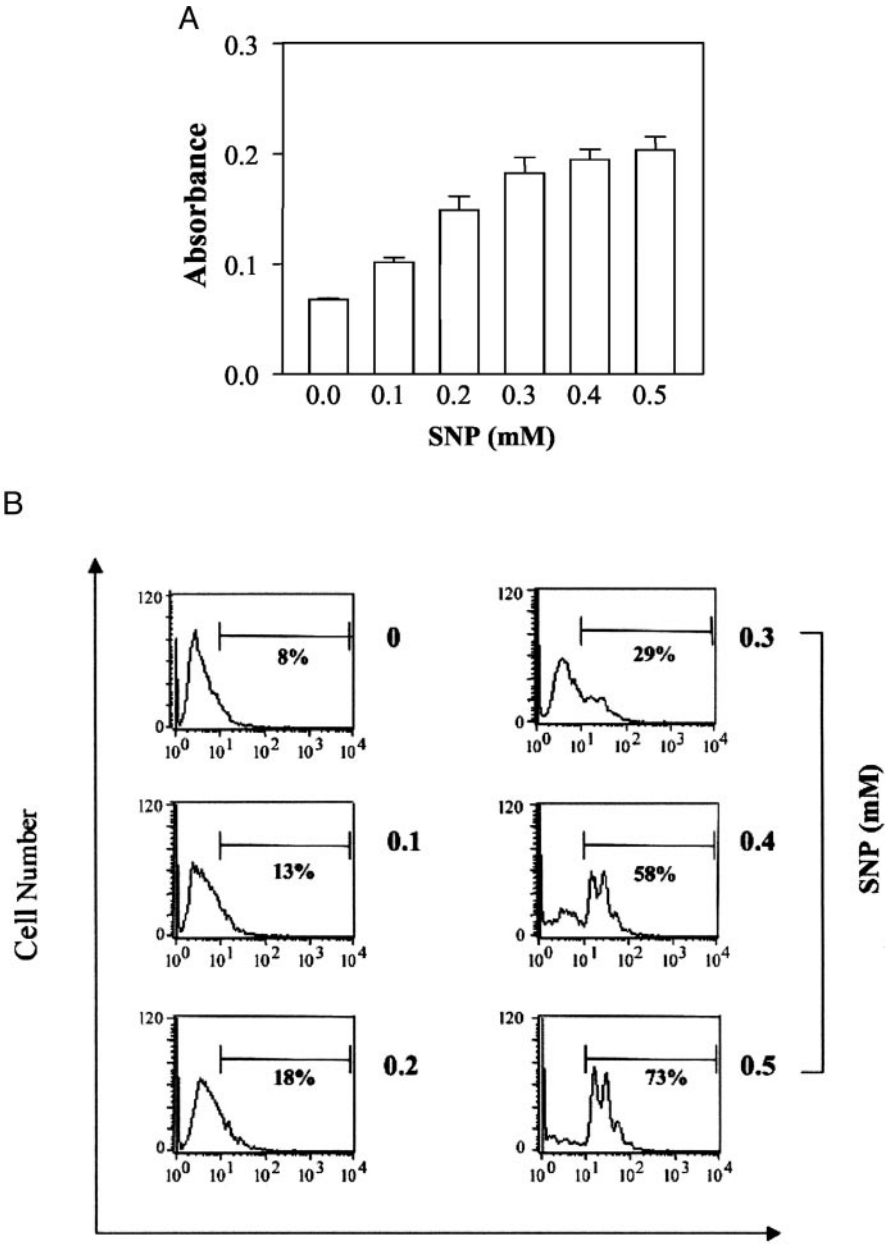

FIG. 1. **SNP-induced RNI and ROS production and apoptotic cell death in the photoreceptor cell line 661W.** 661W cells were treated with increasing concentrations of SNP (0.1–0.5 mM) for 20 h. *A*, the presence of nitric oxide metabolites was detected colorimetrically by the Griess reaction. The *error bars* correspond to the S.D. of three independent experiments done in duplicate. *B*, superoxide anion levels were quantified by flow cytometry using the probe DHE prior to SNP treatment (0 mM) and after treatment with 0.1–0.5 mM SNP. The percentage of cells displaying increased levels of ROS is shown at each SNP concentration. Results are representative of three independent experiments done in duplicate. *C*, cell death measurements were done by flow cytometry using propidium iodide. Dot plots show that treatment of 661W photoreceptor cells with the nitric oxide donor SNP induced oxidative stress, leading to cell death. Results are representative of three independent experiments carried out in duplicate. *FSC-H*, forward-angle light scatter.

apoptosis are still not fully understood, and little is known about oxidative pathways involved in retinal death. Therefore, to gain a better understanding of the events triggered by RNI and ROS in photoreceptors, the 661W cell line was treated with increasing concentrations of the nitric oxide donor SNP (0.1–0.5 mM) for 20 h. Previous studies have shown that SNP can trigger apoptosis in neurons (31). The production of nitric oxide metabolites was detected with the Griess reaction (29). In this method, nitrite metabolites are detected with a colorimetric reaction. Therefore, the value of the resulting absorbance is proportional to the amount of RNI present in the samples. As illustrated in Fig. 1*A*, an increase in nitric oxide metabolites was observed in 661W photoreceptor cells upon treatment with up to a concentration of SNP of 0.3 mM. Higher concentrations of SNP did not significantly modify the concentration of RNI in the cells.

In parallel with this study, superoxide anion formation was monitored using the probe DHE (Fig. 1*B*). Contrary to results observed for RNI, treatment with the lowest concentrations of SNP (0.1–0.2 mM) did not significantly alter the levels of superoxide anions present in 661W cells, and increased levels of ROS were not detected until treatment with 0.3 mM SNP. Incubation with 0.5 mM SNP increased superoxide anion levels up to 73%, indicating a modification of the redox state in 661W cells.

Quantification of cell death was performed by flow cytometric analysis. Propidium iodide was used to quantify the population of cells in which membrane integrity was lost. As expected, treatment of 661W cells with SNP (0.1–0.5 mM) induced cell death, with only 29% of cells surviving post-insult with 0.5 mM SNP (Fig. 1*C*). Nevertheless, an SNP concentration of 0.3 mM, which resulted in ~50% cell death, was chosen for further studies. Apoptotic cell death was then assessed by detection of DNA fragmentation by DNA gel electrophoresis after treatment with 0.3 mM SNP. The presence of the DNA ladder was detected 48 h post-insult (data not shown). In conclusion, these results confirm and extend previous observations showing the involvement of ROS in photoreceptor cell death (11, 12, 16).

661W Photoreceptor Cell Death Induced by SNP Is Mediated by an Increase in Intracellular Ca^{2+} Levels and Calpain Activation—In the cell, oxidative stress induces Ca^{2+} influx from the extracellular environment and efflux from intracellular

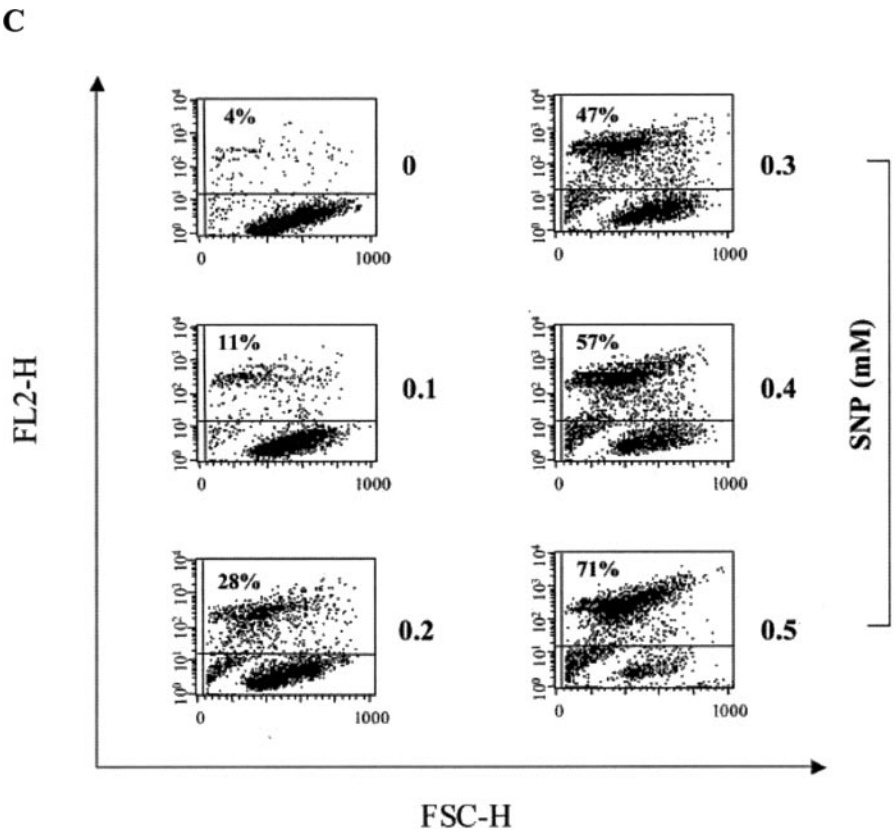

FIG. 1—*continued*

stores, leading to an increase in cytoplasmic Ca^{2+} levels, which has been associated with apoptosis in diverse *in vivo* and *in vitro* systems (32). It has also been shown that elevated cytosolic Ca^{2+} levels play a role in rod photoreceptor apoptosis (11, 33, 34). In this study, intracellular Ca^{2+} levels were determined using the fluorescent probe Fluo-3/acetoxymethyl ester. To ensure that SNP treatment of 661W photoreceptor cells increased $[Ca^{2+}]_i$, calcium levels in untreated 661W cells were compared with those in cells incubated with 0.3 mM SNP for 20 h. As depicted in the histogram in Fig. 2*A*, treatment of 661W cells with 0.3 mM SNP produced an increase in FL1 fluorescence, indicating an increased concentration of intracellular calcium.

Activation of calcium-dependent proteases such as calpains is thought to play an important role in certain models of oxidative stress-induced apoptosis (35–37). In addition, several studies have shown that calpains can contribute to neuronal death (38–40), and calpain inhibitors have been used to block apoptosis (41–43). However, to date, little is known about the involvement of calpains in photoreceptor cell death. Previous work from this laboratory has reported the activation of calpains during light-induced retinal degeneration (12). To verify the activation of calpains in 661W cells following increased levels of intracellular Ca^{2+}, we performed immunoblot analyses using polyclonal antibodies against the calpain isoforms m-calpain and μ-calpain. Moreover, we also analyzed the common small regulatory subunit of calpains, which is dissociated in response to increased levels of cytosolic calcium (44). As illustrated in Fig. 2*B*, a decrease in the total amount of m-calpain was observed after a 24-h treatment of 661W cells with 0.3 mM SNP (50% cell death). The reduction in calpain levels was even more evident after 48 h (76% cell death). Although calpains require only an increase in $[Ca^{2+}]_i$ to become active, the autoproteolytic cleavage further enhanced their activity. Fig. 2*B* shows that SNP-treated 661W cells contained the autolysed form of μ-calpain (78 kDa), indicating that this isoform is also activated by SNP. Consistent with the results of the immunoblot analysis of the latent forms of calpains, a decrease in the intensity of the band corresponding to the calpain small subunit (28 kDa) was observed after 24 h of treatment, whereas after 48 h, the band was not detectable any longer. Western blot analysis of the calpain substrate calpastatin was carried out to confirm the activation of calpains. The complete disappearance of the calpastatin band after 24 h of treatment strongly indicates that calpains are involved in 661W photoreceptor death induced by SNP.

661W Photoreceptor Cell Death Induced by SNP Is Caspase-dependent—It is well documented that caspases are the central executioners of apoptosis in a wide range of cell types (45, 46). Several reports have described a role for caspases during photoreceptor apoptosis (9, 47). Tuohy *et al.* (26) recently reported that apoptosis of 661W photoreceptors triggered by transfecting the Fas-associated death domain is caspase-dependent. In contrast, a lack of caspase activation has also been demonstrated during retinal cell apoptosis (10). Work performed in two *in vivo* models of photoreceptor apoptosis has also shown that light-induced photoreceptor apoptosis and *N*-methyl-*N*-nitrosourea-induced retinal cell apoptosis are caspase-independent (11, 12, 16). Because oxidative stress appears to play a key role in 661W cell death induced by SNP, we determined the activation status of caspase-3, -9, and -12 by Western blot analysis.

Caspase-12 is predominantly found as a proenzyme in the endoplasmic reticulum (ER), and it has been recently demonstrated that this caspase can mediate an ER-specific apoptotic pathway (48). The activation of caspase-12 results from agents or insults that affect ER homeostasis, and it has recently been shown (35) that activation of m-calpain is required for procaspase-12 processing. In view of the fact that we had observed m-calpain activation in SNP-treated 661W cells, we investigated whether caspase-12 is active. Fig. 3*A* demonstrates the presence of two fragments at ~38 kDa in 661W cells treated

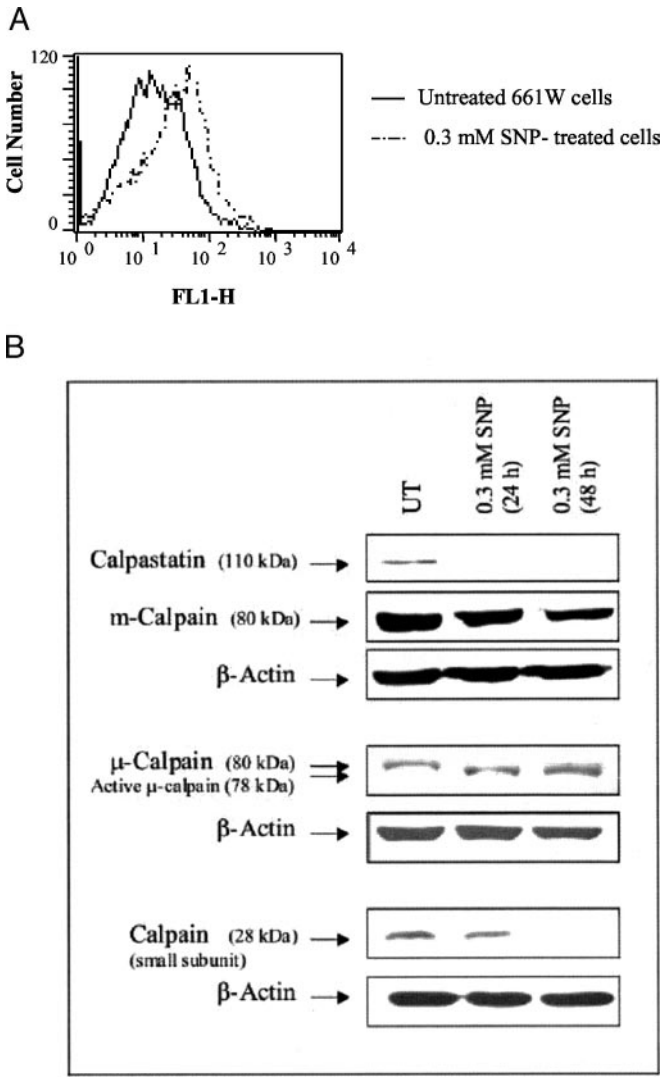

FIG. 2. **Oxidative stress in 661W photoreceptor cells induces increases in intracellular calcium levels and leads to activation of m-calpain.** *A*, intracellular Ca^{2+} levels were monitored using the fluorescent probe Fluo-3/acetoxymethyl ester in untreated 661W cells and in cells incubated with 0.3 mM SNP for 20 h. A shift in the peak to increased fluorescence in the FL1 channel indicates an increased level of intracellular Ca^{2+} in SNP-treated 661W cells. The histogram is representative of three independent experiments done in duplicate. *B*, shown are the results from immunoblot analysis of m- and μ-calpains, their small regulatory subunit (28 kDa), and calpastatin. Western blotting was performed using 661W cell lysates taken prior to SNP insult (untreated (*UT*)) and 24 and 48 h after treatment with 0.3 mM SNP. Polyclonal antibodies were used to detect activation of m- and μ-calpains. The results were confirmed by dissociation of the small subunit and detection of the calpain substrate calpastatin. After 24 and 48 h of treatment, the calpastatin band (110 kDa) could not be detected, suggesting calpain-mediated processing. The blot was reprobed with an antibody to β-actin to demonstrate equal protein loading. Analyses were done in triplicate with similar results.

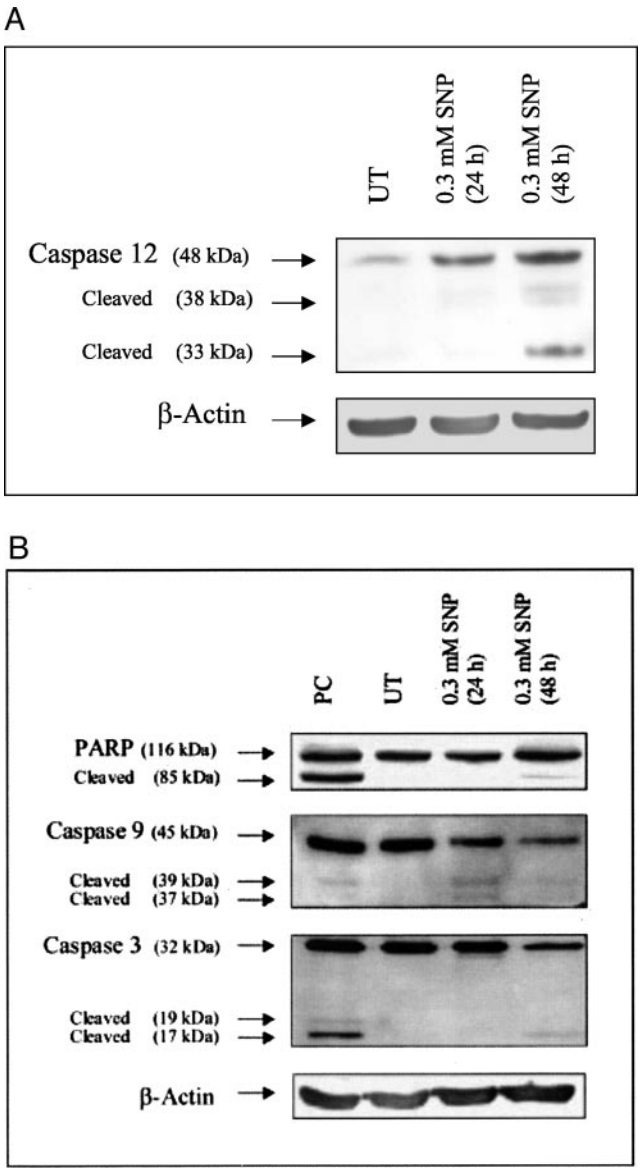

FIG. 3. **Caspase-3, -9, and -12 are activated during 661W photoreceptor apoptosis induced by SNP.** *A*, cell lysates were taken from 661W cells 24 and 48 h after treatment with 0.3 mM SNP. Untreated 661W cells (*UT*) were used as negative control. The presence of 38-kDa bands and a 30–33-kDa fragment in the blot indicates caspase-12 activation. *B*, activation of caspase-3, its substrate poly(ADP-ribose) polymerase (*PARP*), and caspase-9 was analyzed by Western blotting. Untreated 661W cells and 100 nM staurosporine-treated 661W cells (24 h) were used as negative (*UT*) and positive (*PC*) controls, respectively. Procaspase-3 processing was verified after a 48-h treatment with SNP by the presence of the 17-kDa active subunit on the blot. Detection of the 85-kDa PARP fragment confirmed caspase-3 activation. Caspase-9 activation was demonstrated by the presence of its cleaved fragments (39 and 37 kDa) after a 24-h treatment of 661W cells with 0.3 mM SNP. All blots were reprobed with an antibody to β-actin to demonstrate equal protein loading. A representative result of three experiments is shown on all immunoblots.

with a concentration of SNP of 0.3 mM for 24 h. The level of these fragments was increased at 48 h, and also an additional fragment appeared at 30/33 kDa at this time point. Moreover, an increase in the level of full-length caspase-12 could be observed in both time points. Although the molecular mass of the active subunits of caspase-12 has not been precisely described, previous work has referred to protein fragments at ~35 kDa as an indication of caspase-12 activation by m-calpain (35). Therefore, our results indicate that caspase-12 is active in SNP-treated 661W photoreceptor cells.

Caspase-9 is activated in response to stimuli that lead to cytochrome *c* release from mitochondria and is essential for initiation of the caspase cascade, involving caspase-2, -3, -6, and -7 (49). Nitric oxide has been reported to induce mitochondrial permeability transition, which is supposed to cause the liberation of apoptogenic factors from mitochondria (50, 51). In our case, the elevated ROS levels detected in SNP-treated 611W cells suggested a mitochondrial dysfunction. Therefore, to determine whether caspase-9 is active or inactive in our system, 661W photoreceptor cells were incubated with 0.3 mM SNP for 24 and 48 h prior to Western blot analysis. 661W cells

treated with 100 nM staurosporine for 24 h were used as positive controls. The tyrosine kinase inhibitor staurosporine has been shown to induce apoptosis in 661W cells following a mitochondrial pathway in which caspase-3, -7, and -9 are active.[2] The concentration of staurosporine was chosen to give a similar percentage cell death as seen for 0.3 mM SNP. Caspase-9 is synthesized as a 45-kDa inactive proenzyme and is cleaved to generate active subunits of 39 and 37 kDa. The presence of the 39- and 37-kDa caspase-9 fragments after a 24-h incubation of 611W photoreceptor cells with a concentration of SNP of 0.3 mM demonstrated the activation of caspase-9 (Fig. 3*B*).

Caspase-3 is considered the main executioner of apoptosis, and the involvement of this enzyme in photoreceptor apoptosis has been reported (47, 52, 53). Caspase-3 is synthesized as a 32-kDa proenzyme that requires cleavage by caspase-9 to its 17–19-kDa active subunits (49). As shown in Fig. 3*B*, the presence of cleaved caspase-3 fragments was not detected in 661W cells after a 24-h treatment with 0.3 mM SNP. At this time point, the Western blot revealed only a 29-kDa band under the procaspase-3 unit. This fragment has been recently identified as the cleaved product of procaspase-3 by m-calpain (54), which supports our previous observations as previous results shown in this work (Fig. 2*B*) suggesting that calpains are active in SNP-induced photoreceptor apoptosis. After 48 h, the 17-kDa active subunit of caspase-3 was visible on the blot, indicating classical caspase-3 activation. This result demonstrates that cleavage of procaspase-3 is a late event in the signaling cascade triggered by SNP. The results from Western blot analysis show that activation of calpains and caspase-9 took place 24 h earlier, before processing of the executioner caspase-3 was detected. To confirm caspase-3 activation, cleavage of the caspase-3 substrate PARP was analyzed by Western blotting. PARP can be cleaved by either calpains or caspase-3. A polyclonal antibody was used to detect both PARP and the 85-kDa fragment resulting from caspase-3 cleavage (55). According to the results obtained for caspase-3, the 85-kDa inactive subunit of PARP was present only after a 48-h treatment with SNP (Fig. 3*B*). In summary, the results obtained in the Western blot analysis demonstrate that signaling mediated by both calpains and caspases may be involved in SNP-induced 661W photoreceptor apoptosis. This is the first demonstration that both caspases and calpains are involved in photoreceptor apoptosis.

The Broad-range Caspase Inhibitor Z-VAD-fmk Cannot Inhibit SNP-induced Apoptosis in 661W Photoreceptor Cells—Caspase inhibitors have been employed to block apoptosis in cell systems in which caspases have a central role. In view of the fact that SNP-induced apoptosis in 661W cells was caspase-dependent, we examined the effect of Z-VAD-fmk on photoreceptor apoptosis. Therefore, 661W cells were preincubated with Z-VAD-fmk prior to treatment with 0.3 mM SNP; and subsequently, caspase-3 activity was analyzed by cleavage of the colorimetric substrate Ac-DEVD-*p*NA. As depicted in Fig. 4*A*, preincubation of 661W cells with Z-VAD-fmk completely prevented caspase-3 activation due to SNP treatment. However, a parallel determination of cell death in those samples (Fig. 4*B*) revealed that despite Z-VAD-fmk inhibition of caspase-3, the pan-caspase inhibitor was unable to prevent SNP-induced apoptosis in 661W photoreceptor cells. Moreover, the cell death percentage estimated for Z-VAD-fmk-pretreated 661W cells was significantly higher than that exhibited by those photoreceptors that had not been preincubated with the caspase inhibitor (61 and 53%, respectively). We have demonstrated that both caspases and calpains are involved in photoreceptor apoptosis. Therefore, our findings suggest that inhibition of caspases in SNP-treated 661W photoreceptor cells activates a more harmful death pathway, not necessarily apoptotic, in which calpains could be the main executioners. Consistent with this hypothesis, immunoblot analysis of m-calpain and its small subunit in SNP-treated samples revealed that the pan-caspase inhibitor Z-VAD-fmk did not inhibit calpain activity; on the contrary, a slight increase in m-calpain activation was observed under these conditions compared with samples treated with only SNP, and no difference was observed in the dissociation of the small regulatory subunit of calpain (Fig. 4*C*). In view of these results, alternatives other than caspase inhibitors have to be found to inhibit apoptosis in 661W photoreceptor cells.

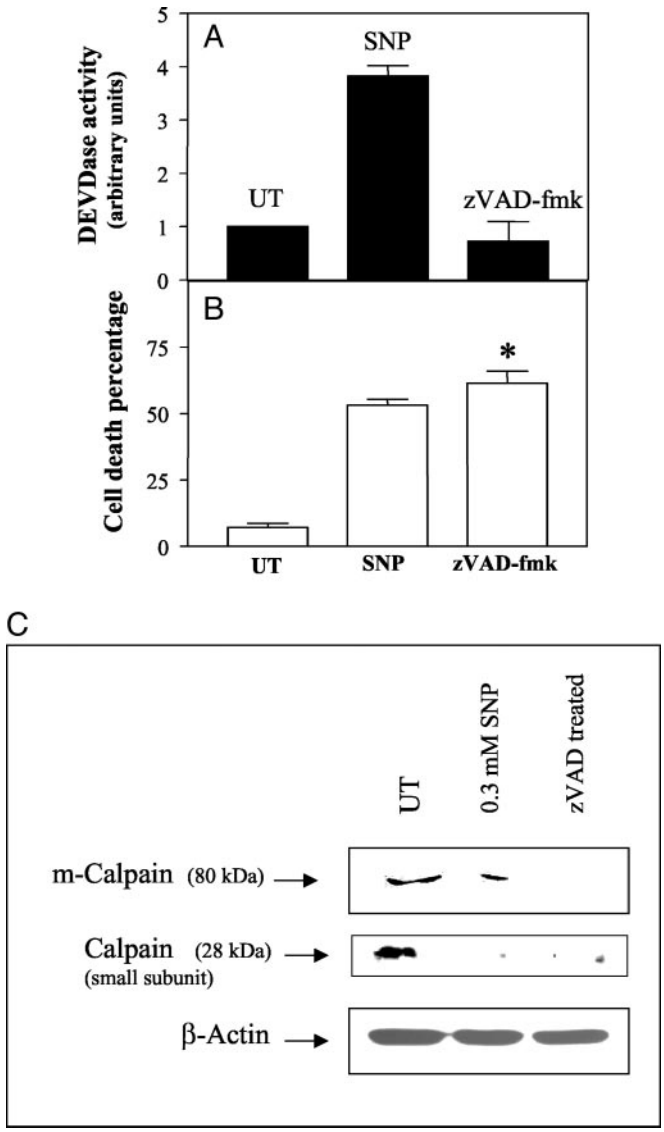

FIG. 4. **The caspase inhibitor Z-VAD-fmk inhibits SNP-triggered DEVD-like caspase-3 activity in 661W photoreceptor cells but cannot prevent 661W cell apoptosis.** The photoreceptor cell line 661W was incubated with 50 μM Z-VAD-fmk for 1 h before treatment with 0.3 mM SNP. Untreated (*UT*) and SNP-treated 661W cells were used as negative and positive controls, respectively. *A*, Ac-DEVD-*p*NA hydrolysis was monitored after a 24-h incubation at 37 °C and quantified colorimetrically at 405 nm. Results are expressed in arbitrary units (absorbance of the sample divided by the absorbance of the UT cells). *, significant difference compared with SNP-treated cells (*t* test; $p < 0.05$). *B*, cell death measurements were done by flow cytometry using propidium iodide. *Error bars* correspond to the S.D. of three independent experiments carried out in duplicate. *C*, immunoblot analysis of m-calpain and its small regulatory subunit (28 kDa) shows increased calpain activity in 661W cells pretreated with Z-VAD-fmk.

[2] V. Gómez-Vicente and T. G. Cotter, unpublished data.

CR-6 Acts as a Scavenger of ROS and Reduces Cell Death in 661W Photoreceptor Cells Induced by SNP—CR-6 could be envisaged as a simple tocopherol analog. In addition to a phenol moiety, its structure contains two non-substituted and highly activated aromatic positions that confer upon the molecule the ability to react with radical species. Thus, the capacity of CR-6 to react with nitrating species such as NO and $ONOO^-$ has already been demonstrated; moreover, CR-6 has been shown to prevent glutamate neurotoxicity in primary cultures of cerebellar neurons by scavenging NO (27). Therefore, CR-6 appealed to us as a worthwhile candidate to study the effect of pretreatment with an antioxidant molecule on 661W cell death induced by SNP since we had already observed that RNI and ROS were involved in 661W cell apoptosis. 661W cells were preincubated for 15 min with increasing concentrations of CR-6 (0.2–100 μM). Then, 0.3 mM SNP was added to the wells, and incubation was continued for 20 h. A significant reduction in cell death was observed when 661W cells were pretreated with high concentrations of CR-6 (100 to 12.5 μM). Thus, after a 15-min incubation with 25 μM CR-6 cell death was reduced in 63% of the cells. Moreover, the protecting capacity exhibited by CR-6 in 661W cells was superior to that of other assessed antioxidants (butylated hydroxytoluene, resveratrol, ascorbic acid, and *N*-acetyl-L-cysteine) and similar to that of α-tocopherol (data not shown). As a result of this study, a CR-6 concentration of 25 μM was chosen for further assays. We then tested whether CR-6 prevents cell death when 661W cells are incubated with increasing concentrations of SNP. We also assessed whether CR-6 acts as a scavenger of radical species. As depicted in Fig. 1*A*, the presence of nitric oxide metabolites was determined colorimetrically using the Griess reaction, whereas the generation of superoxide anions was monitored using the probe DHE. Fig. 5*A* illustrates the results of these experiments. As shown in *panel a*, preincubation of 661W cells with 25 μM CR-6 significantly prevented cell death at all concentrations of SNP studied. It should be noted that the percentage of cell death was reduced to basal levels in those samples pretreated with CR-6 and preincubated with 0.1 and 0.2 mM SNP. Therefore, CR-6 confers complete protection against apoptosis induced by low concentrations of SNP in 661W photoreceptor cells under the conditions tested. In the rest of the samples, the protection achieved varied from 70 to 50% when cells were insulted with 0.3 and 0.5 mM SNP, respectively. *Panel b* illustrates the reduction of superoxide anion levels in all samples that had been pretreated with CR-6, although the decrease in the ROS levels was more significant at high concentrations of SNP (46 and 40% reduction for samples pretreated with 25 μM CR-6 and incubated with 0.4 and 0.5 mM SNP, respectively). The ability of CR-6 to scavenge superoxide anions has not been described previously. However, previous work has demonstrated that CR-6 exhibits a potent inhibitory activity of lipid peroxidation induced in rat liver microsomes, which could constitute evidence of ROS scavenging by CR-6 (56). Moreover, it has been suggested that scavenging of ROS could have been a contribution to the protective effect exhibited by CR-6 in primary cultures of cerebellar neurons (27). *Panel c* illustrates the presence of nitrites in 661W control cells treated with increasing concentrations of SNP and in those pretreated with CR-6. Surprisingly, an increase in nitrites was detected in all cases. Initially, a decrease in RNI would have been expected if CR-6 had trapped these radicals. However, despite the increased levels of nitrites observed, scavenging of RNI by CR-6 cannot be discarded since the increase in nitrite concentration could be the result of the reaction between CR-6 and nitric oxide or peroxynitrites.

Annexin V staining of 661W cells clearly showed that treatment with 0.3 mM SNP for 20 h was enough to increase phosphatidylserine exposure at the surface of the cell compared with untreated cells (Fig. 5*B*). Dot plots from the fluorescence-activated cell sorter analysis of annexin V-stained cells are divided in four different quadrants. The *lower quadrants* show those cells not stained with propidium iodide, *i.e.* with intact membranes. The *lower left quadrants* show the annexin V-negative propidium iodide-negative population, whereas the *lower right quadrants* shows the annexin V-positive propidium iodide-negative cell population. The *upper quadrants* display cells that have lost membrane integrity and have become propidium iodide-positive. The percentages of cell counts in the *lower quadrants* are indicated with *numbers*. Thus, in *panel a* (untreated cells), the annexin V-negative propidium iodide-negative cell population counts for 89% of the whole cells, whereas only 5% of the total cell population is annexin V-positive. Treatment with 0.3 mM SNP for 20 h shifted the annexin V-positive population to 15.2% (*panel b*). Nevertheless, a 15 min-incubation of 661W cells with 25 μM CR-6 was enough to completely reverse the annexin V-positive percentage to 4.6% (*panel c*). Therefore, under these conditions, CR-6 confers substantial protection against SNP-induced phosphatidylserine exposure.

CR-6 Can Reduce Increases in Intracellular Calcium Levels and Prevent m-calpain Activation in 661W Photoreceptor Cells Treated with SNP—We have shown above that oxidative stress in 661W cells due to treatment with SNP led to an increase in cytosolic Ca^{2+} levels, which subsequently activated calpains. Since CR-6 traps ROS, reducing the oxidative stress in SNP-treated cells, we considered it worthwhile to investigate the downstream effects that scavenging of ROS by CR-6 could have in SNP-treated 661W photoreceptors. Thus, the cytosolic Ca^{2+} levels were measured in control cells (cells treated for 20 h) and in cells pretreated with 25 μM CR-6 for 15 min. As expected, CR-6 partially inhibited the increase observed in intracellular Ca^{2+} levels induced by SNP treatment at all concentrations analyzed (Fig. 6*A*). Although oxidative stress has been described as one of the causes of increased $[Ca^{2+}]_i$ in the cell, other agents can generate an increase in intracellular Ca^{2+} concentration as well. For example, Bcl-2 family proteins, in addition to other apoptotic factors such as activated caspases, may also have control over the Ca^{2+} levels in cells (57, 58). This fact suggests that other agents could be involved in the increased calcium concentration observed in SNP-treated 661W cells and could explain why CR-6 scavenging of ROS cannot completely reduce the intracellular calcium concentration to its basal level, at least at the lowest concentrations of SNP tested.

To investigate whether CR-6 can prevent calcium-mediated calpain activation, control cell samples treated with 0.3 mM SNP for 24 and 48 h were compared with cell samples incubated with 25 μM CR-6 for 15 min by Western blot analysis. Fig. 6*B* shows that CR-6 pretreatment of 661W cells prevented m-calpain activation since 661W photoreceptors incubated with CR-6 did not show the 58-kDa band corresponding to active m-calpain. To ensure that CR-6 prevents calpain activation, we studied the extent of calpastatin cleavage in 661W cells pretreated with CR-6 before insult with SNP. As illustrated in Fig. 6*B*, CR-6 completely abolished calpastatin cleavage when 661W photoreceptors were treated with SNP for 24 h. At 48 h, CR-6 only partially attenuated calpastatin cleavage. These results correlate very well with previous observations. After a 24-h treatment with 0.3 mM SNP, the 661W cell death percentage was 50%. Pretreatment of photoreceptors with CR-6 prevented cell death by 70%. However, at the 48-h time point, the cell death percentage was comparable with that caused by 0.5 mM SNP treatment; and under these conditions, cell death could be prevented only by 49%.

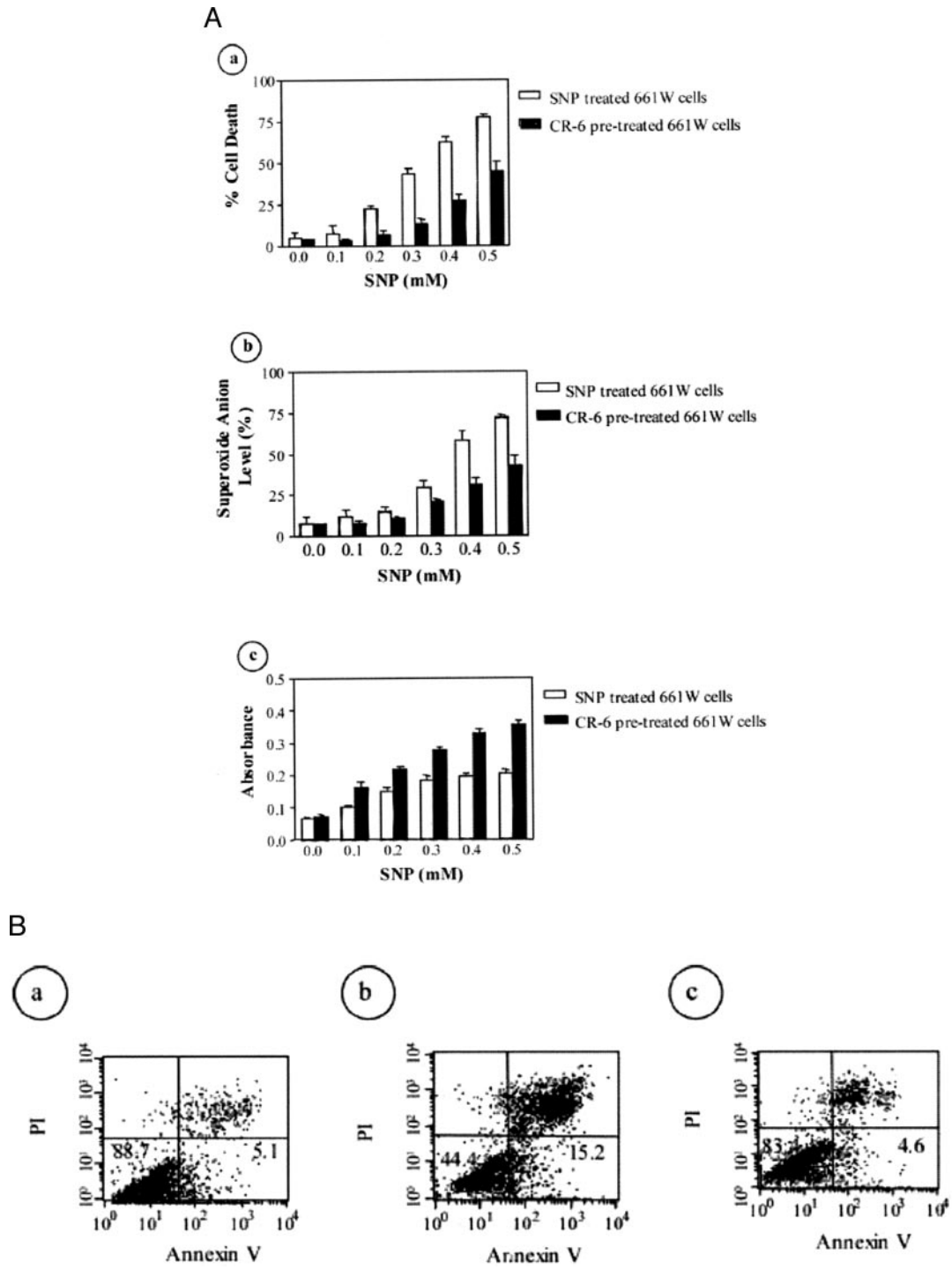

FIG. 5. **Pretreatment of 661W photoreceptor cells with CR-6 inhibits apoptosis induced by the NO donor SNP.** *A*, 661W control cells were treated with dose-dependent concentrations of SNP (0.1–0.5 mM) for 20 h (*white bars*). CR-6-pretreated cells were incubated for 15 min with a 25 μM concentration of the antioxidant before insult (*black bars*). CR-6 significantly reduced cell death induced by SNP at all concentrations studied (*panel a*) due to the scavenging of superoxide anions (*panel b*). Results correspond to three different experiments done in duplicate; *error bars* indicate the S.D. *B*, shown are the results from flow cytometric analysis of untreated 661W cells (*panel a*), 661W control cells treated with 0.3 mM SNP for 20 h (*panel b*), and 661W cells pretreated with 25 μM CR-6 before SNP insult (*panel c*) and stained with annexin V and propidium iodide (*PI*). *Numbers* in the corresponding quadrants indicate the percentage of cells present in the area. A reduction in the percentage of the annexin V-positive population in those cells pretreated with CR-6 indicates the protective effect conferred by the antioxidant against phosphatidylserine exposure. The fluorescence-activated cell sorter analysis was repeated three times with similar results.

CR-6 Prevents Caspase-12 Processing while Partially Inhibiting Caspase-3 and Caspase-9 Cleavage—The observation that CR-6 prevented m-calpain cleavage led us to assay whether caspase-12 processing is inhibited as well. Immunoblotting was performed with 661W control photoreceptors (0.3 mM SNP insult for 24 and 48 h) and with those pretreated with 25 μM CR-6 (Fig. 7*A*). As expected, since m-calpain activated caspase-12, pretreatment of 661W cells with CR-6 also prevented caspase-12 activation. The 33-kDa cleavage band observed after treatment with 0.3 mM SNP for 24 h was not visible when 661W photoreceptors were incubated with the antioxidant CR-6. Moreover, the increased intensity of the procaspase-12 band at the 24-h time point compared with the untreated cells was completely restored to basal levels in CR-6-pretreated

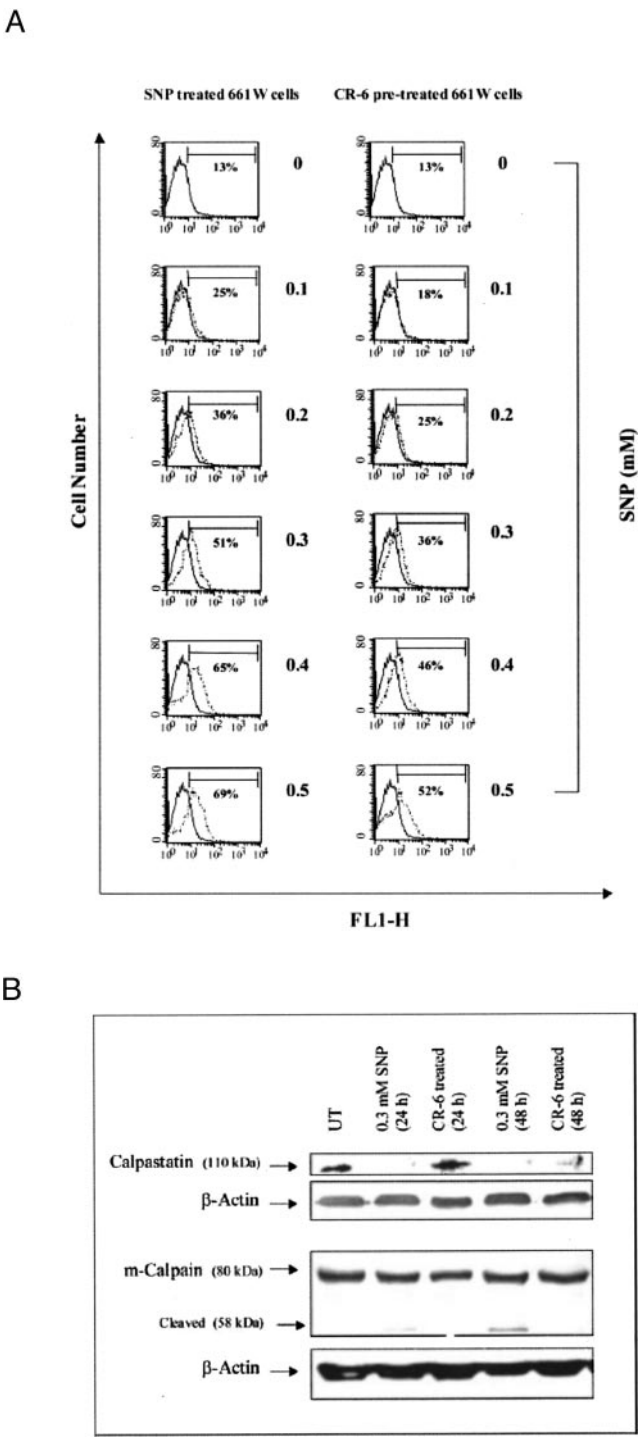

FIG. 6. **Effect of CR-6 on increased intracellular calcium levels and calpain activation induced by SNP in 661W photoreceptor cells.** *A*, intracellular Ca^{2+} levels were measured using the fluorescent probe Fluo-3 in untreated cells (0 mM SNP; *solid lines*), in control cells treated with dose-dependent concentrations of SNP (0.1–0.5 mM; *dotted lines* in *left panels*), and in cells pretreated with 25 μM CR-6 for 15 min before insult with the corresponding SNP concentration (*dotted lines* in *right panels*). The percentage of cells that showed increased Ca^{2+} levels in 661W photoreceptor cells induced by SNP treatment is indicated in each panel. The histograms in the *right panels* illustrate the partial inhibition of intracellular Ca^{2+} increases by CR-6. A representative result of three experiments is shown. *B*, shown are the results from immunoblot analysis of m-calpain and its substrate calpastatin in 661W control cells and in cells pretreated with 25 μM CR-6. Western blotting was performed using equivalent quantities of total protein from 661W cell lysates taken prior to SNP insult (untreated (*UT*)) and 24 and 48 h after treatment with 0.3 mM SNP. The results show that m-calpain activation could be prevented by pretreatment with CR-6. Results are representative of three experiments.

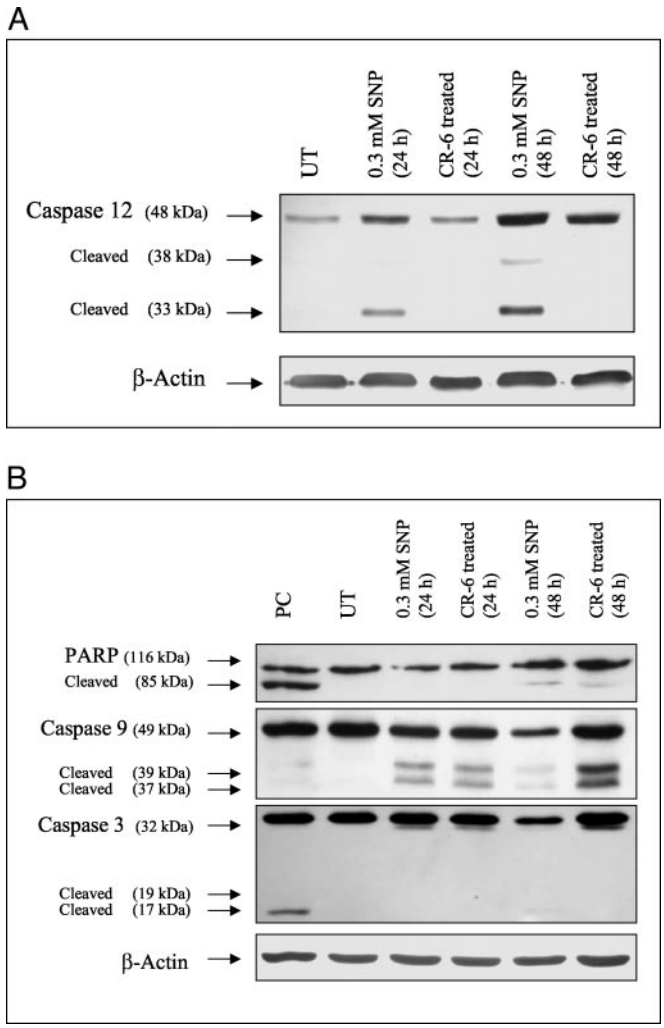

FIG. 7. **Effect of CR-6 on caspase-3, -9, and -12 activation status in SNP-treated 661W photoreceptor cells.** *A*, procaspase-12 processing was prevented by preincubating 661W photoreceptor cells with the antioxidant CR-6 before insult with SNP. Cell lysates were taken from 661W cells 24 and 48 h after treatment with 0.3 mM SNP. Untreated 661W cells (*UT*) were used as a negative control. *B*, CR-6 only partially inhibited caspase-3 and caspase-9 activation. 661W cells treated with 100 nM staurosporine for 24 h were used as a positive control (*PC*). The presence of the cleaved caspase-9 fragments (39 and 37 kDa) when SNP-treated 661W cells were preincubated with 25 μM CR-6 demonstrates that the antioxidant could not prevent procaspase-9 processing. Accordingly with these results, caspase-3 activation was not inhibited by CR-6 either. All blots were reprobed with an antibody to β-actin to demonstrate equal protein loading. A representative result of three experiments is shown on all immunoblots. *PARP*, poly(ADP-ribose) polymerase.

photoreceptors. At 48 h, CR-6 also completely prevented caspase-12 processing. Both the 33- and 38-kDa cleavage bands were not present in 661W cells incubated with the antioxidant. However, the basal levels of procaspase-12 were not completely restored in this case, indicating that some stress was still present under these conditions.

Following the analysis of caspase-12, we proceeded with the study of the activation state of caspase-3 and caspase-9 when SNP-treated 661W photoreceptors were preincubated with CR-6 before insult. Fig. 7*B* illustrates the results obtained. Activation of caspase-9 could not be prevented by CR-6, and only at the 48-h time point could a slight recovery be observed in the levels of the procaspase-9 band. According to the results observed with caspase-9, caspase-3 activation was not prevented by CR-6 pretreatment of 661W cells. As seen for caspase-9, only a partial inhibition of procaspase-3 cleavage

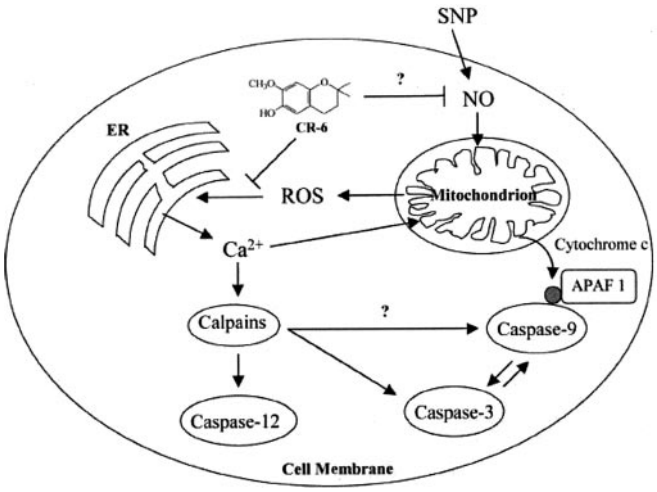

FIG. 8. **Schematic representation of the hypothetical events that take place distal to treatment of 661W photoreceptor cells with SNP.** The nitric oxide donor SNP induces mitochondrial permeability transition, which can cause release of apoptogenic factors such as cytochrome *c*. Caspase-9 activation following apoptosome formation leads to processing of downstream caspases. Simultaneously, the oxidative stress generated by the SNP insult affects ER homeostasis, which is reflected in increased intracellular calcium levels. The calcium-dependent protease m-calpain is then activated. Subsequently, caspase-12 processing occurs. Altogether, these events lead to the apoptotic death of 661W photoreceptor cells. The activation of the calpain-mediated apoptotic pathway can be prevented by CR-6, which has been demonstrated to scavenge ROS in SNP-treated 661W photoreceptors. *APAF 1*, apoptotic protease-activating factor-1.

was observed at the 48-h time point. The results obtained for the caspase-3 substrate PARP agree with our previous observations. The 85-kDa cleavage band was still present at the 48-h time point after pretreatment of 661W cells with CR-6. These results indicate that the calpain-mediated apoptotic pathway in 661W photoreceptors induced by SNP may run independently from the mitochondrial pathway and that CR-6 scavenging of ROS can prevent only the events triggered in the ER (Fig. 8).

DISCUSSION

Oxidative Stress Generated by the Nitric Oxide Donor SNP Induces in 661W Photoreceptor Cells Apoptotic Programmed Death in Which Calpains and Caspases Are Involved—In this study, we have explored the molecular events occurring after induction of oxidative stress in 661W photoreceptor cells by treatment with the nitric oxide donor SNP. Nitric oxide has been reported to inhibit cytochrome oxidase, the terminal enzyme of the mitochondrial electron transport chain, leading to the production of superoxide anions that can activate cell death mechanisms (59). For example, it has been shown that nitric oxide triggers cell death in neurons and that apoptotic events are mediated by ROS (13, 60). In the same context, previous work performed in this laboratory with an animal model has also demonstrated that NO has a key role in retinal degeneration and that an early and rapid increase in intracellular ROS accompanies retinal cell apoptosis *in vivo* (11). The data presented in this work are in agreement with previous observations and demonstrate that SNP induces ROS production in 661W photoreceptor cells, which activates the apoptotic cascade, leading to cell death.

Elevation of cytosolic Ca^{2+} levels has been reported to be a key event in apoptosis (32). Studies performed in isolated rat retinas have demonstrated that Ca^{2+} overload can induce mitochondrial depolarization and subsequently the release of apoptosis-inducing factors (such as cytochrome *c*), which lead to the sequential activation of caspase-9 and caspase-3 (34). Preventing apoptosis in photoreceptors using calcium channels blockers (12, 33) and calcium antagonist (61) has confirmed these observations. In this study, intracellular calcium levels were monitored after insult with dose-dependent concentrations of SNP. An increase in the concentration of cytosolic calcium was determined at every concentration of SNP studied (Fig. 2*A* and 6*B*). Moreover, we noted that the increase observed in the Ca^{2+} level correlated with the percentage of photoreceptor death.

Calpains are calcium-dependent proteases that have been proposed to participate in apoptosis. Calpain activation during apoptosis has been observed both in *in vitro* and *in vivo* systems (35, 36, 42, 62) Recently, a role for calpains in PC12 cell apoptosis due to oxidative stress and increased calcium levels has been demonstrated (36). However, to date little, is known about the importance of calpains in retinal apoptosis, and the molecular events they induce in photoreceptor cells have not yet been defined. The results presented in this work provide evidence of the contribution of calpains to photoreceptor apoptosis. We have shown that calcium overload activated both m- and μ-calpains in SNP-treated 661W photoreceptor cells (Fig. 2*B*). The dissociation of the small subunit of calpains, the processing of the endogenous calpain inhibitor calpastatin, and the truncation of procaspase-3 to a 29-kDa polypeptide (54) have further supported the role of calpains in SNP-induced 661W photoreceptor apoptosis.

It has been demonstrated that photoreceptor cells from adult mice can undergo caspase-independent cell death *in vivo* (10, 11). However, this study has illustrated that the caspase machinery is activated in 661W photoreceptor cells after insult with SNP (Fig. 3). This apparent contradiction may be explained by the fact that in adult mice there is a significant reduction in the expression of caspase-3 and caspase-9. Furthermore, it has been shown the protein levels of apoptotic protease-activating factor-1 also decrease with aging (12). This can be the key reason why caspase-independent apoptosis is seen in the retinas of these animals. Retinas from newborn animals still express caspases and can undergo caspase-dependent apoptosis. The 661W cell line is derived from the retinas of 8-day postnatal mice. It is reasonable to expect the caspase pathway to be active in SNP-treated 661W cells. In addition, it has been reported that the nature and severity of an insult determine whether apoptosis is caspase-dependent or -independent (63). It is reasonable to conclude then that photoreceptors are capable of caspase-dependent and -independent cell death, with the initial insult and aging shaping the cellular response. On the other hand, this study has shown for the first time that photoreceptor cells can undergo an apoptotic programmed death in which calpains and caspases are involved. There is growing evidence of cross-talk between caspases and calpains, and it has been reported that calpain can mediate the cleavage of caspase-3, -7, -8, -9, and -12 (35, 39, 54, 62, 64). We have shown that inhibition of m-calpain prevented caspase-12 activation. The processing of procaspase-3 by m-calpain was suggested by the presence of the 29-kDa fragment in 661W cells 24 h post-insult with SNP.

CR-6 Acts as a Scavenger of ROS and Reduces 661W Photoreceptor Cell Death Induced by SNP by Preventing the Activation of the Calpain-mediated Apoptotic Pathway—This study has shown that even though the broad-spectrum caspase inhibitor Z-VAD-fmk prevented caspase-3 activation, it could not inhibit SNP-induced 661W photoreceptor apoptosis (Fig. 4). The fact that also calpains participated in 661W cell apoptosis and were still active in the presence of Z-VAD-fmk (Fig. 4*C*) could explain why the inactivation of caspases did not lead to inhibition of apoptosis. On the other hand, the results pre-

sented in this work demonstrate that CR-6 reduced apoptosis induced by SNP in 661W photoreceptor cells (Fig. 5*A*, *panel a*). Our results show that incubation of 661W cells with CR-6 prior to insult resulted in a decrease in superoxide anion levels, indicating that CR-6 behaved as a ROS scavenger in our system (Fig. 5*A*, *panel b*), which emphasizes the critical role of ROS in photoreceptor apoptosis. In addition, CR-6 has been demonstrated to have a very low toxicity in 661W photoreceptor cells (data not shown), which makes it an ideal candidate as a potential therapeutic agent.

The downstream effects that CR-6 could have in SNP-treated 661W photoreceptors were investigated. In this section of the study, we have shown that CR-6 scavenging of intracellular ROS led to a reduction in the increased cytosolic calcium levels induced by SNP treatment (Fig. 6*A*). The decrease observed in the intracellular Ca^{2+} concentration was reflected in m-calpain inactivation (Fig. 6*B*), which in turn inhibited procaspase-12 processing (Fig. 7*A*). Therefore, CR-6 has been demonstrated to be a useful tool to reduce oxidative stress-induced apoptosis in 661W cells and has allowed us to show the important role played by calpains in photoreceptor apoptosis. Despite the inhibitory effect elicited by CR-6 in the calpain-mediated apoptotic pathway, CR-6 scavenging of ROS could not prevent the activation of the caspase-mediated mitochondrial pathway. Only partial prevention of procaspase processing was observed, most likely as a consequence of m-calpain inhibition (Fig. 7*B*). In conclusion, the data presented here provide a possible mechanism by which oxidative stress mediates apoptosis in 661W photoreceptor cells (Fig. 8). Moreover, our findings suggest a central role for both caspases and calpains in the apoptotic process. We have also shown that the inhibition of caspases triggers an alternative mechanism of cell death in 661W cells and that only prevention of calpain activation leads to a reduction of 661W photoreceptor apoptosis induced by SNP.

REFERENCES

1. Kaufmann, S. H., and Hengartner, M. O. (2001) *Trends Cell Biol.* **11,** 526–534
2. Ferri, K. F., and Kroemer, G. (2001) *Nat. Cell Biol.* **3,** E255–E263
3. Migliore, L., and Coppede, F. (2002) *Mutat. Res.* **512,** 135–153
4. Olinski, R., Gackowski, D., Foksinski, M., Rozalski, R., Roszkowski, K., and Jaruga, P. (2002) *Free Radic. Biol. Med.* **33,** 192–200
5. Chang, G. Q., Hao, Y., and Wong, F. (1993) *Neuron* **11,** 595–605
6. Li, Z., and Milan, A. (1995) in *Degenerative Diseases of the Retina* (Anderson, R. M. L., and Hollyfield, J., eds) Plenum Publishing Corp., New York
7. Dunaief, J. L., Dentchev, T., Ying, G. S., and Milam, A. H. (2002) *Arch. Ophthalmol.* **120,** 1435–1442
8. Carella, G. (2003) *Eur. J. Ophthalmol.* **3,** S5–S10
9. Liu, C., Li, Y., Peng, M., Laties, A. M., and Wen, R. (1999) *J. Neurosci.* **19,** 4778–4785
10. Carmody, R. J., and Cotter, T. G. (2000) *Cell Death Differ.* **7,** 282–291
11. Donovan, M., Carmody, R. J., and Cotter, T. G. (2001) *J. Biol. Chem.* **276,** 23000–23008
12. Donovan, M., and Cotter, T. G. (2002) *Cell Death Differ.* **9,** 1220–1231
13. Okuno, S., Shimizu, S., Ito, T., Nomura, M., Hamada, E., Tsujimoto, Y., and Matsuda, H. (1998) *J. Biol. Chem.* **273,** 34272–34277
14. Zhang, X., Chen, J., Graham, S. H., Du, L., Kochanek, P. M., Draviam, R., Guo, F., Nathaniel, P. D., Szabo, C., Watkins, S. C., and Clark, R. S. (2002) *J. Neurochem.* **82,** 181–191
15. Selznick, L. A., Zheng, T. S., Flavell, R. A., Rakic, P., and Roth, K. A. (2000) *J. Neuropathol. Exp. Neurol.* **59,** 271–279
16. Doonan, F., Donovan, M., and Cotter, T. G. (2003) *J. Neurosci.* **23,** 5723–5731
17. Liang, F. Q., and Godley, B. F. (2003) *Exp. Eye Res.* **76,** 397–403
18. Carmody, R. J., McGowan, A. J., and Cotter, T. G. (1999) *Exp. Cell Res.* **248,** 520–530
19. Crawford, M. J., Krishnamoorthy, R. R., Rudick, V. L., Collier, R. J., Kapin, M., Aggarwal, B. B., Al-Ubaidi, M. R., and Agarwal, N. (2001) *Biochem. Biophys. Res. Commun.* **281,** 1304–1312
20. Krishnamoorthy, R. R., Crawford, M. J., Chaturvedi, M. M., Jain, S. K., Aggarwal, B. B., Al-Ubaidi, M. R., and Agarwal, N. (1999) *J. Biol. Chem.* **274,** 3734–3743
21. Lam, S., Tso, M. O., and Gurne, D. H. (1990) *Arch. Ophthalmol.* **108,** 1751–1757
22. Ranchon, I., Gorrand, J. M., Cluzel, J., Droy-Lefaix, M. T., and Doly, M. (1999) *Investig. Ophthalmol. Vis. Sci.* **40,** 1191–1199
23. Rosner, M., Lam, T. T., Fu, J., and Tso, M. O. (1992) *Arch. Ophthalmol.* **110,** 857–861
24. Al-Ubaidi, M. R., Font, R. L., Quiambao, A. B., Keener, M. J., Liou, G. I., Overbeek, P. A., and Baehr, W. (1992) *J. Cell Biol.* **119,** 1681–1687
25. Roque, R. S., Rosales, A. A., Jingjing, L., Agarwal, N., and Al-Ubaidi, M. R. (1999) *Brain Res.* **836,** 110–119
26. Tuohy, G., Millington-Ward, S., Kenna, P. F., Humphries, P., and Farrar, G. J. (2002) *Investig. Ophthalmol. Vis. Sci.* **43,** 3583–3589
27. Montoliu, C., Llansola, M., Saez, R., Yenes, S., Messeguer, A., and Felipo, V. (1999) *Biochem. Pharmacol.* **58,** 255–261
28. Casas, J., Gorchs, G., Sanchez-Baeza, F., Teixidor, P., and Messeguer, A. (1992) *J. Agric. Food Chem.* **40,** 585–590
29. Marzinzig, M., Nussler, A. K., Stadler, J., Marzinzig, E., Barthlen, W., Nussler, N. C., Beger, H. G., Morris, S. M., Jr., and Bruckner, U. B. (1997) *Nitric Oxide* **1,** 177–189S. M. J.
30. Gorman, A., McGowan, A., and Cotter, T. G. (1997) *FEBS Lett.* **404,** 27–33
31. Tamatani, M., Ogawa, S., Nunez, G., and Tohyama, M. (1998) *Cell Death Differ.* **5,** 911–919
32. Berridge, M. J., Bootman, M. D., and Lipp, P. (1998) *Nature* **395,** 645–648
33. Frasson, M., Sahel, J. A., Fabre, M., Simonutti, M., Dreyfus, H., and Picaud, S. (1999) *Nat. Med.* **5,** 1183–1187
34. He, L., Poblenz, A. T., Medrano, C. J., and Fox, D. A. (2000) *J. Biol. Chem.* **275,** 12175–12184
35. Nakagawa, T., and Yuan, J. (2000) *J. Cell Biol.* **150,** 887–894
36. Ray, S. K., Fidan, M., Nowak, M. W., Wilford, G. G., Hogan, E. L., and Banik, N. L. (2000) *Brain Res.* **852,** 326–334
37. O'Donovan, C. N., Tobin, D., and Cotter, T. G. (2001) *J. Biol. Chem.* **276,** 43516–43523
38. McCollum, A. T., Nasr, P., and Estus, S. (2002) *J. Neurochem.* **82,** 1208–1220
39. Neumar, R. W., Xu, Y. A., Gada, H., Guttmann, R. P., and Siman, R. (2003) *J. Biol. Chem.* **278,** 14162–14167
40. Rami, A. (2003) *Neurobiol. Dis.* **13,** 75–88
41. Jordan, J., Galindo, M. F., and Miller, R. J. (1997) *J. Neurochem.* **68,** 1612–1621
42. Rami, A., Agarwal, R., Botez, G., and Winckler, J. (2000) *Brain Res.* **866,** 299–312
43. McGinnis, K. M., Whitton, M. M., Gnegy, M. E., and Wang, K. K. (1998) *J. Biol. Chem.* **273,** 19993–20000
44. Pal, G. P., Elce, J. S., and Jia, Z. (2001) *J. Biol. Chem.* **276,** 47233–47238
45. Thornberry, N. A., and Lazebnik, Y. (1998) *Science* **281,** 1312–1316
46. Nicholson, D. W. (1999) *Cell Death Differ.* **6,** 1028–1042
47. Jomary, C., Neal, M. J., and Jones, S. E. (2001) *Mol. Cell. Neurosci.* **18,** 335–346
48. Nakagawa, T., Zhu, H., Morishima, N., Li, E., Xu, J., Yankner, B. A., and Yuan, J. (2000) *Nature* **403,** 98–103
49. Slee, E. A., Harte, M. T., Kluck, R. M., Wolf, B. B., Casiano, C. A., Newmeyer, D. D., Wang, H. G., Reed, J. C., Nicholson, D. W., Alnemri, E. S., Green, D. R., and Martin, S. J. (1999) *J. Cell Biol.* **144,** 281–292
50. Hortelano, S., Dallaporta, B., Zamzami, N., Hirsch, T., Susin, S. A., Marzo, I., Bosca, L., and Kroemer, G. (1997) *FEBS Lett.* **410,** 373–377
51. Vieira, H. L., Belzacq, A. S., Haouzi, D., Bernassola, F., Cohen, I., Jacotot, E., Ferri, K. F., El Hamel, C., Bartle, L. M., Melino, G., Brenner, C., Goldmacher, V., and Kroemer, G. (2001) *Oncogene* **20,** 4305–4316
52. Wu, J., Gorman, A., Zhou, X., Sandra, C., and Chen, E. (2002) *Investig. Ophthalmol. Vis. Sci.* **43,** 3349–3354
53. Kim, D. H., Kim, J. A., Choi, J. S., and Joo, C. K. (2002) *Ophthalmic Res.* **34,** 150–157
54. Blomgren, K., Zhu, C., Wang, X., Karlsson, J. O., Leverin, A. L., Bahr, B. A., Mallard, C., and Hagberg, H. (2001) *J. Biol. Chem.* **276,** 10191–10198
55. Tewari, M., Quan, L. T., O'Rourke, K., Desnoyers, S., Zeng, Z., Beidler, D. R., Poirier, G. G., Salvesen, G. S., and Dixit, V. M. (1995) *Cell* **81,** 801–809
56. Irurre, J. J., Casas, J., Ramos, I., and A., M. (1993) *Bioorg. Med. Chem.* **1,** 219–225
57. Hajnoczky, G., Davies, E., and Madesh, M. (2003) *Biochem. Biophys. Res. Commun.* **304,** 445–454
58. Ermak, G., and Davies, K. J. (2002) *Mol. Immunol.* **38,** 713–721
59. Moncada, S., and Erusalimsky, J. D. (2002) *Nat. Rev. Mol. Cell. Biol.* **3,** 214–220
60. Yuyama, K., Yamamoto, H., Nishizaki, I., Kato, T., Sora, I., and Yamamoto, T. (2003) *J. Neurosci. Res.* **73,** 351–363
61. Yamazaki, H., Ohguro, H., Maeda, T., Maruyama, I., Takano, Y., Metoki, T., Nakazawa, M., Sawada, H., and Dezawa, M. (2002) *Investig. Ophthalmol. Vis. Sci.* **43,** 919–926
62. Ruiz-Vela, A., González de Buitrago, G., and Martínez-A, C. (1999) *EMBO J.* **18,** 4988–4998
63. Nicotera, P. (2002) *Toxicol. Lett.* **127,** 189–195
64. Chua, B. T., Guo, K., and Li, P. (2000) *J. Biol. Chem.* **275,** 5131–5135